

Electronic Supplementary Material to: Understanding the Development of the 2018/19 Central Pacific El Niño*

Chengyang GUAN¹, Xin WANG^{2,3,4}, and Haijun YANG⁵

¹College of Ocean Science and Engineering, Shandong University of Science and Technology, Qingdao 266590, China

²State Key Laboratory of Tropical Oceanography, South China Sea Institute of Oceanology,
Chinese Academy of Sciences, Guangzhou 510301, China

³Southern Marine Science and Engineering Guangdong Laboratory (Guangzhou), Guangzhou 511458, China

⁴Innovation Academy of South China Sea Ecology and Environmental Engineering,
Chinese Academy of Sciences, Guangzhou 510301, China

⁵Department of Atmospheric and Oceanic Sciences, Fudan University, Shanghai 200433, China

ESM to: Guan, C. Y., X. Wang, and H. J. Yang, 2023: Understanding the development of the 2018/19 central Pacific El Niño. *Adv. Atmos. Sci.*, **40**(1), 177–185, <https://doi.org/10.1007/s00376-022-1410-1>.

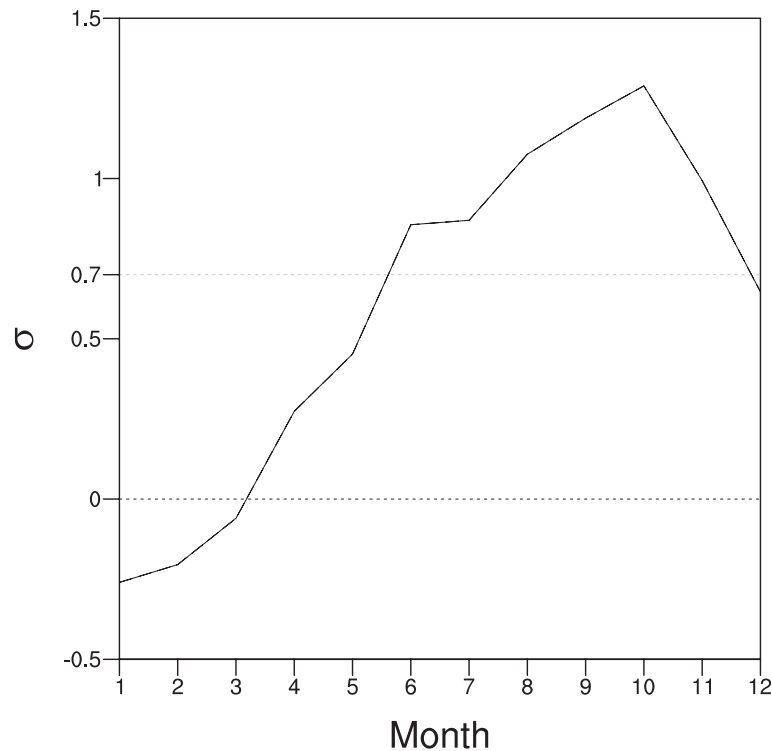


Fig. S1. El Niño Modoki index (EMI) in 2018 relative to the climatological standard deviation.

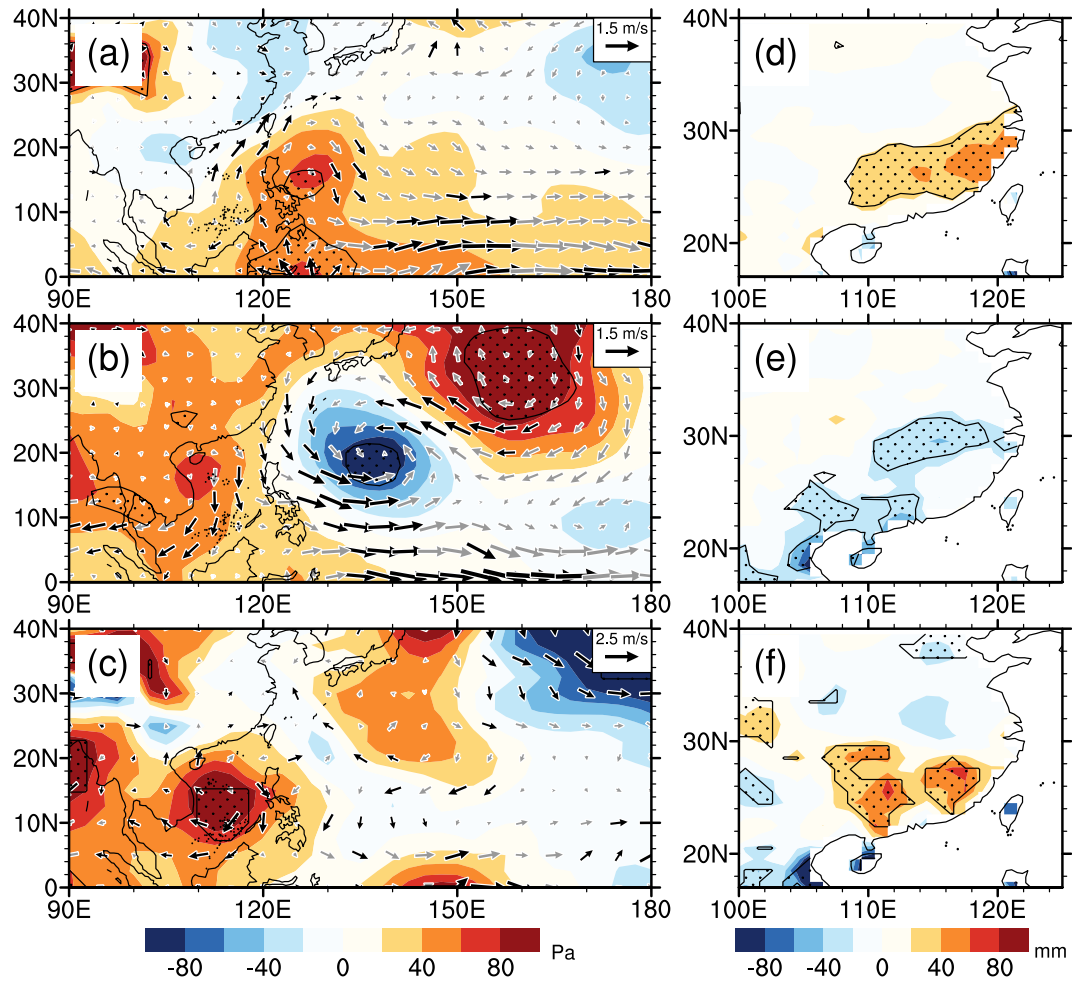


Fig. S2. (a) Anomalies of SLP (shading) and sea surface wind (vector) in the developing Sep–Oct–Nov (SON) of the CP-I El Niño (a), CP-II El Niño (b), and 2018/19 El Niño (c). (d–f) Precipitation anomalies in southern China at the same time. Black dots in (a), (b), (d), and (e) indicate areas exceeding the 90% confidence level. Black dots in (c) and (f) indicate areas exceeding ± 1 standard deviation. Black vectors in (a) and (b) indicate areas exceeding the 90% confidence level. Black vectors in (c) indicate areas exceeding ± 1 standard deviation.

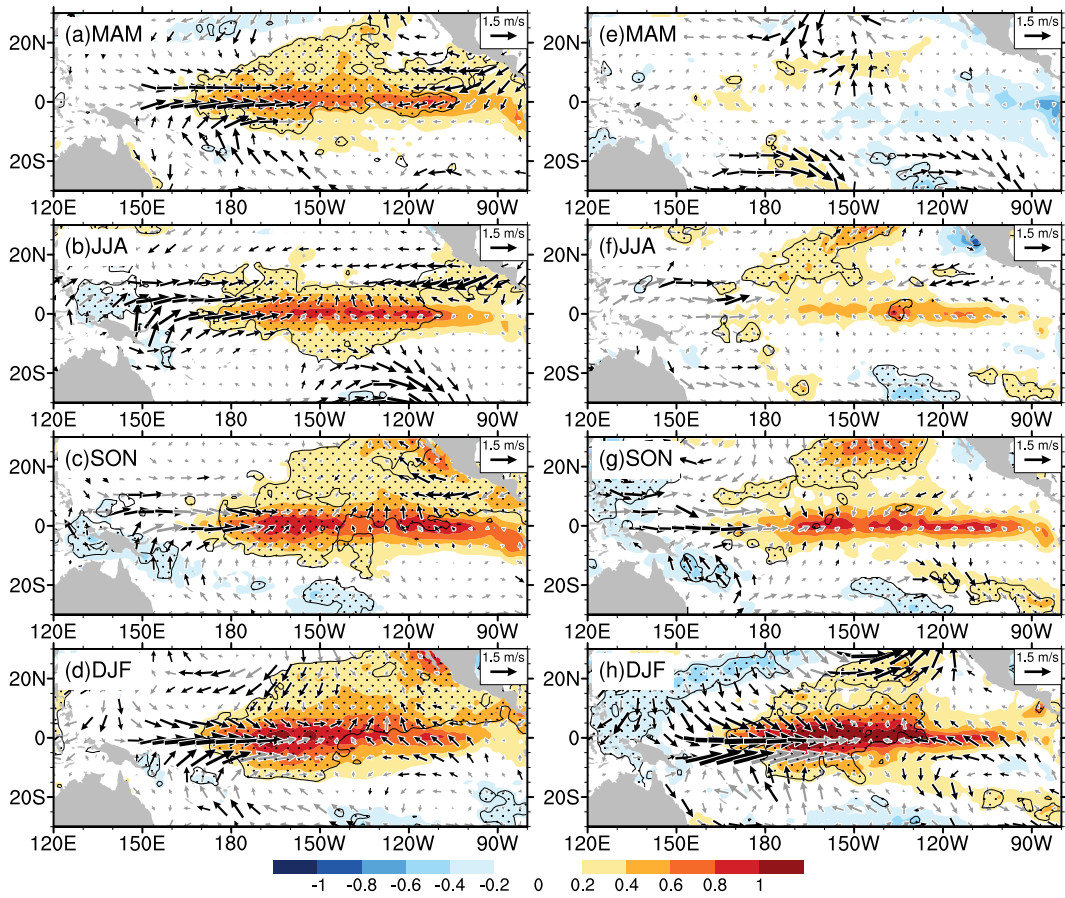


Fig. S3. Evolution of SST (shading, units: $^{\circ}\text{C}$) and wind (vector) anomalies in the tropical Pacific during the development of the CP-I (a–d) and CP-II (e–h) El Niño. Black vectors indicate wind anomalies exceeding the 90% confidence level. Dotted areas indicate where SST anomalies exceed the 90% confidence level.

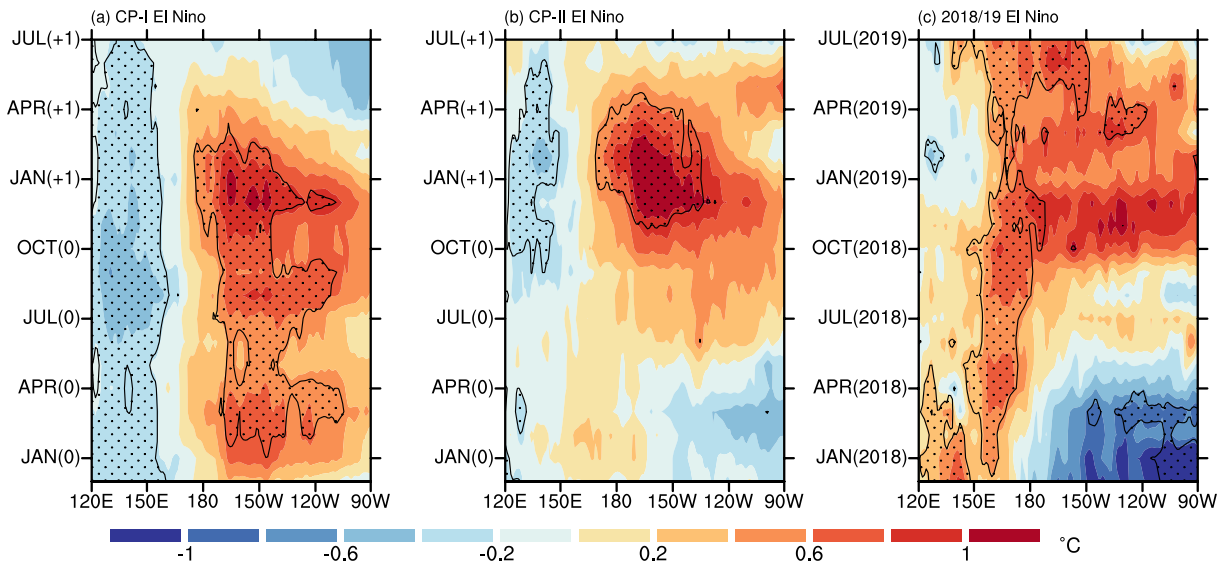


Fig. S4. Evolutions of SST anomalies in the equatorial Pacific (averaged between 5°S–5°N) during the (a) CP-I El Niño, (b) CP-II El Niño, and (c) 2018/19 El Niño. In (a) and (b), (0) and (+1) on the y-axis indicate the developing and decaying year, respectively. Black dots in (a) and (b) denote areas exceeding the 90% confidence level. Black dots in (c) denote areas exceeding ± 1 standard deviation.

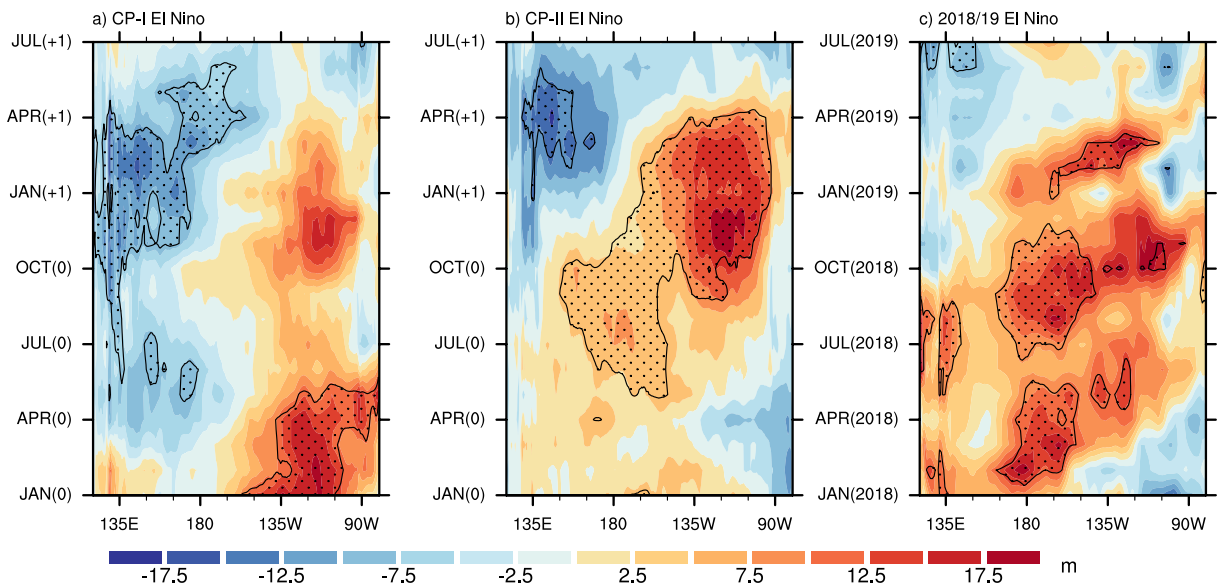


Fig. S5. Evolutions of thermocline anomalies in the equatorial Pacific (averaged between 5°S–5°N) during the (a) CP-I El Niño, (b) CP-II El Niño, and (c) 2018/19 El Niño. In (a) and (b), (0) and (+1) on the y-axis indicate the developing and decaying year, respectively. Black dots in (a) and (b) denote areas exceeding the 90% confidence level. Black dots in (c) denote areas exceeding ± 1 standard deviation.

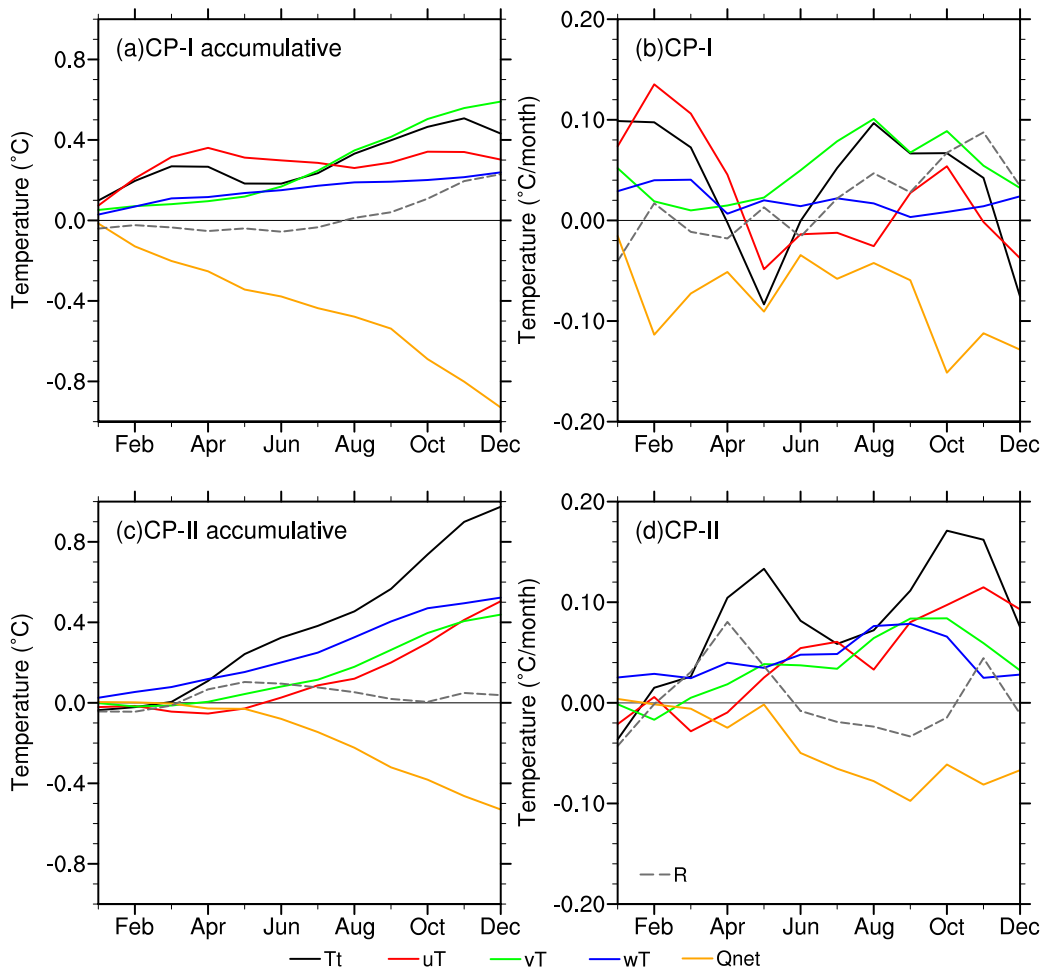


Fig. S6. Ocean mixed-layer heat budget analysis of Niño-4 region during the development of the (b) CP-I El Niño and (d) CP-II El Niño. (a) and (c) illustrate the accumulative contributions of each term in (b) and (d), respectively. T_t represents the temperature tendency. uT , vT , and wT represent the zonal, meridional, and vertical advective feedback, respectively. Q_{net} represents the net surface flux. R represents the residuals.

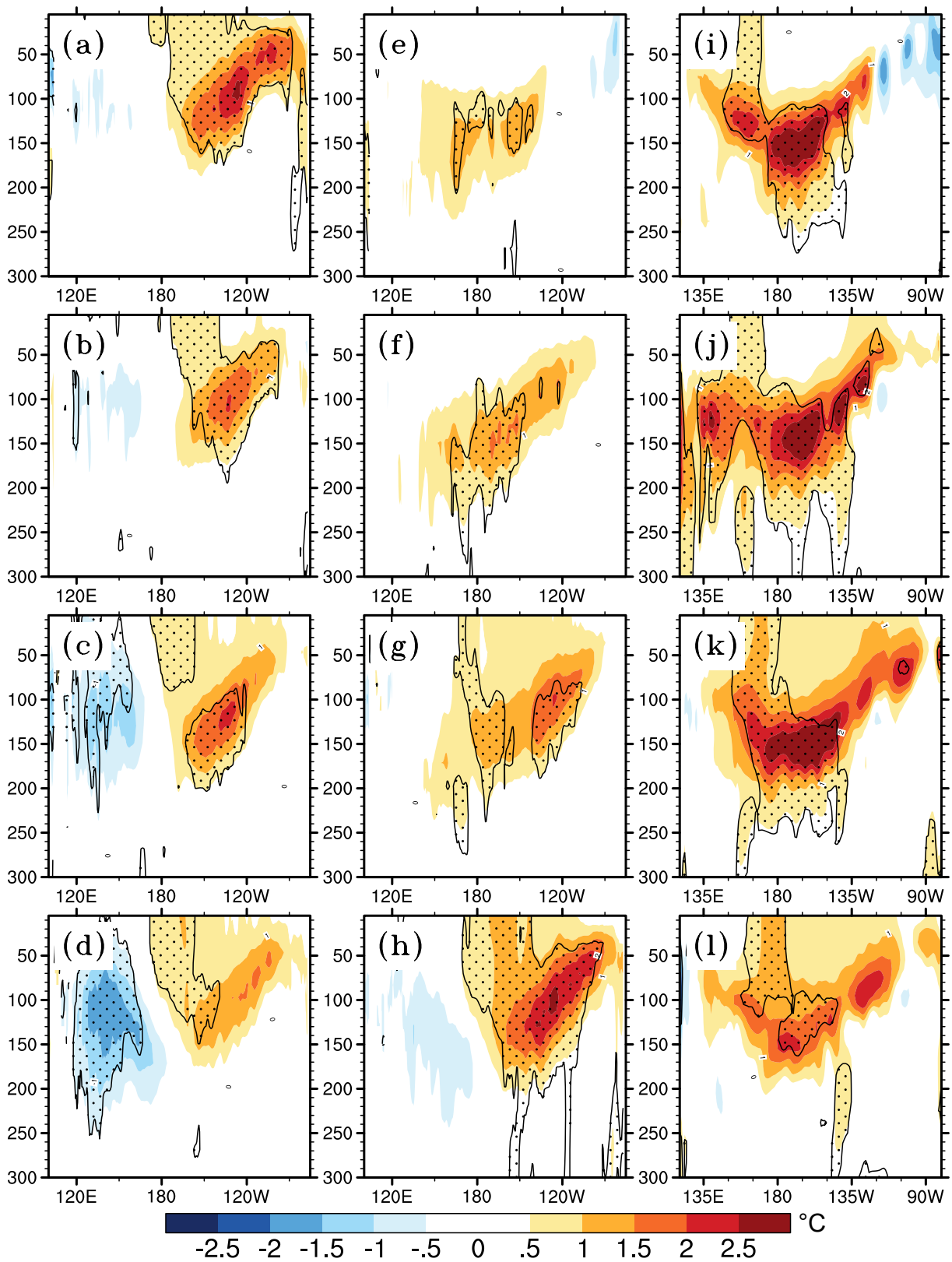


Fig. S7. Depth–longitude section of seasonal averaged subsurface ocean temperature anomalies over the equatorial Pacific (5°S–5°N) in MAM (first row), JJA (second row), SON (third row), and DJF (fourth row) of the developing year for the CP-I (left column), CP-II (middle column), and 2018/19 El Niño (right column). Dotted areas indicate temperature anomalies exceeding the 90% confidence level in (a–h), and those exceeding ± 1 standard deviation in (i–l). Note that the ocean temperature data for the CP-I and CP-II (2018/19) El Niño are from SODA 2.2.4 (GODAS).

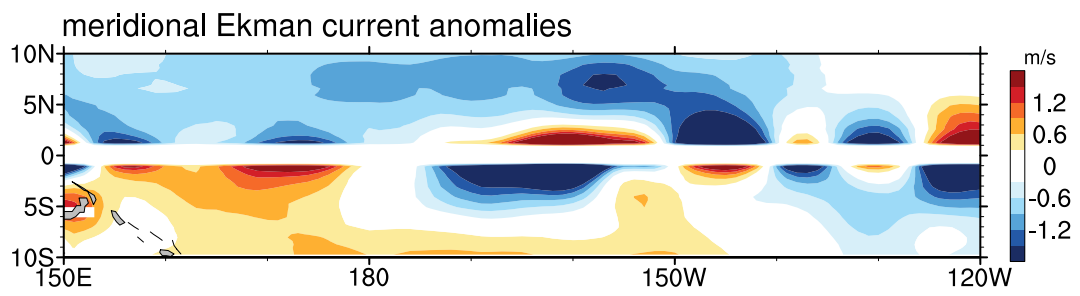


Fig. S8. Meridional Ekman current anomalies induced by the zonal wind stress anomalies during JJA 2018.